AJNR

MR imaging of epidermoid cysts.

D Tampieri, D Melanson and R Ethier

MR Imaging of Epidermoid Cysts

Donatella Tampieri[1]
Denis Melanson
Roméo Ethier

Nine patients with epidermoid cysts, five of them pathologically proved, were evaluated with MR imaging. Six patients also had CT. The cases were reviewed to evaluate the MR appearance of epidermoid cysts and to compare the MR findings with those of CT. The epidermoid cysts demonstrated low-signal intensity on T1-weighted MR images and hyperintensity on T2-weighted images. In five cases the cysts appeared heterogeneously iso- to hyperintense on the intermediate echo, and were surrounded by a thin rim of high signal intensity, which we believe was caused by encased CSF. The CT scans showed the cysts as low-density, well-demarcated lesions that do not enhance after infusion with contrast material.

We conclude that MR is superior to CT in the evaluation of epidermoid cysts and is particularly useful in surgical planning.

Epidermoid cysts, known as "pearly tumors" because of the appearance of their outer surface, are rare lesions that account for approximately 0.2–1.0% of all intracranial tumors. On CT they appear as homogeneous, low-density lesions that are fairly well delineated and do not enhance after infusion with contrast material. Although this CT description is well documented [1–6], the MR appearance of these tumors is not as well known. We reviewed the MR findings of nine patients with the radiologic diagnosis of epidermoid tumor and compared these results with CT studies to identify the characteristics of this tumor that would allow a specific diagnosis.

Materials and Methods

Nine patients, six males and three females, ages 11 to 63 years old, were referred for MR imaging. The MR studies were done on Philips Gyroscan 0.5-T (two cases) and 1.5-T (seven cases) units.

Sagittal and, eventually, coronal T1-weighted images, 550/30/2 (TR/TE/excitations), were obtained in four patients. In all cases, axial, coronal, and, as needed, sagittal views with 2100/30,60 (TR/first-echo TE, second-echo TE), were acquired. The slice thickness varied between 5 and 8 mm, with a 0.5-mm gap; the matrix was 256 × 256. In six cases, a correlative CT study was available. The CT examinations were done in the axial plane with 10-mm slice thickness. In one case, a vertebral angiogram was also obtained.

In five patients, the diagnosis of epidermoid cyst was confirmed pathologically. In one patient, who did not have surgery, CT cisternography was available (Table 1).

Results

On CT, the epidermoid cysts appeared hypodense with no evidence of enhancement after infusion with contrast material. In none of our cases were calcifications or peritumoral edema observed. While the CT findings were similar in all cases, on MR the epidermoid cysts presented some peculiar characteristics (Table 2). In the T1-weighted images (four cases) the epidermoid cysts always had a low-intensity

TABLE 1: Summary of the Cases: Their Location and Surgical Confirmation

Case No.	Age	Gender	MR	CT	Angiogram	Location	Pathology
1	11	M	Yes	No	No	Right cerebellopontine angle cistern	No
2	22	M	Yes	No	No	Right choroidal fissure	No
3	26	F	Yes	Yes	Yes	Fourth ventricle	Yes
4	27	F	Yes	Yes	No	Suprasellar cistern	No (confirmed with CT cisternography)
5	31	M	Yes	Yes	No	Prepontine cistern	No
6	43	M	Yes	No	No	Dumbell type (the cyst was extending from the middle to the posterior cranial fossa)	Yes
7	53	M	Yes	Yes	No	Fourth ventricle	Yes
8	58	F	Yes	Yes	No	Left cerebellopontine angle and prepontine cisterns	Yes
9	63	M	Yes	Yes	No	Dumbell type (the cyst was extending from the middle to the posterior cranial fossa)	Yes

TABLE 2: MR Findings

Case No.	T1-Weighted Image (550/30)	Intermediate Echo (2100/30)	Hyperintense Rim	Second Echo (2100/60)
1	–	Inhomogeneously intense signal	Yes	High-intensity signal
2	–	Low-intensity signal	No	High-intensity signal
3	–	Isointense signal (0.5 T)	No	High-intensity signal
4	Low-intensity signal	Low-intensity signal	No	High-intensity signal
5	Low-intensity signal	Isointense signal	No	High-intensity signal
6	Low-intensity signal	Inhomogeneously intense signal	Yes	High-intensity signal
7	Low-intensity signal	Inhomogeneously intense signal	Yes	High-intensity signal
8	–	Inhomogeneously intense signal (0.5 T)	Yes	High-intensity signal
9	–	Inhomogeneously intense signal	Yes	High-intensity signal

signal caused by their long T1 relaxation time. Nevertheless, their signal was not as hypointense as that of CSF (Fig. 1). In the intermediate-echo images (2100/30), the lesions had an isointense signal in two cases and a hypointense signal in another two cases. In the remaining five cases, the epidermoid cysts showed some specific characteristics on the 2100/30 images. The tumors presented a heterogeneous signal, as a mixture of hypo- and isointense signals, and they were surrounded by a thin and regular smooth rim of high-intensity signal. In the second echo (2100/60), the signal from the tumor became hyperintense in all the cases of our series. The thin rim of high-intensity signal, as observed in the intermediate echo, was not visualized with this sequence, probably because of the masking effect caused by the brightness of the tumor itself; however, both scanners (0.5-T and 1.5-T) allowed the visualization of the high-intensity thin rim in the intermediate echo (Figs. 2 and 3).

The tumors were always located close to the skull base. In three cases the lesions were in the posterior fossa, the prepontine, and the cerebellopontine angle cisterns, respectively. In two patients, the tumors were in the middle cranial fossa, and in one of these cases the tumor extended into the suprasellar region. A dumbell appearance was observed in two cases in which the tumors extended from the middle to the posterior cranial fossa. In two cases, the epidermoid cysts were located in the fourth ventricle with an inferior extension into the vallecular (Fig. 4). MR also allowed the assessment of the tumor's behavior, showing how the cysts tend to fill all

Fig. 1.—Case 4.
A, CT-cisternography shows hypodense suprasellar component of tumor surrounded by opacified CSF. There was no visible filling of the mass by water-soluble contrast material.
B, Coronal MR image (550/30) shows epidermoid cyst surrounding tip of left internal carotid artery without obstructing it. Intensity signal of lesion is less hypointense than that of CSF.
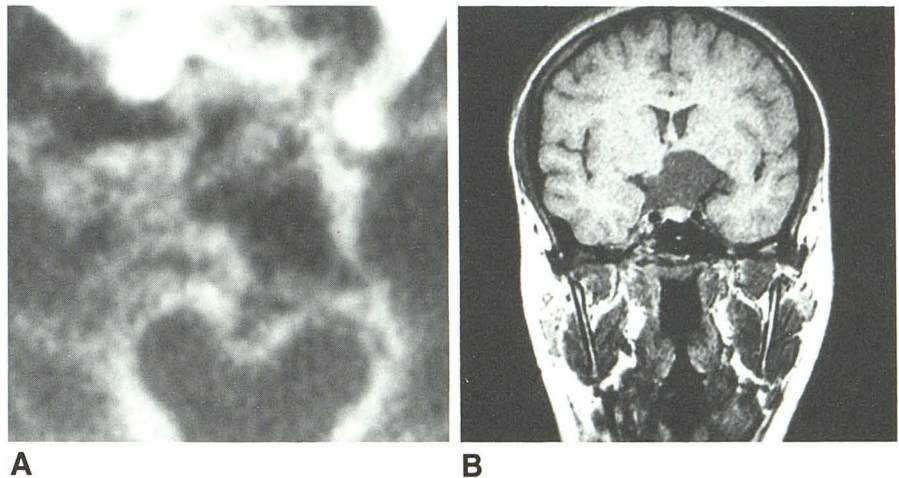

A

B

Fig. 2.—Case 6: epidermoid cyst located in left middle cranial fossa.
A, In this intermediate-echo image (2100/30), the cyst presents an inhomogeneous signal surrounded by a thin rim of high-intensity signal, which we hypothesize is caused by encased CSF around the tumor.
B, In this second-echo image (2100/60), the signal from lesion becomes hyperintense. Thin rim of high-intensity signal is not visualized because of brightness of tumor itself.
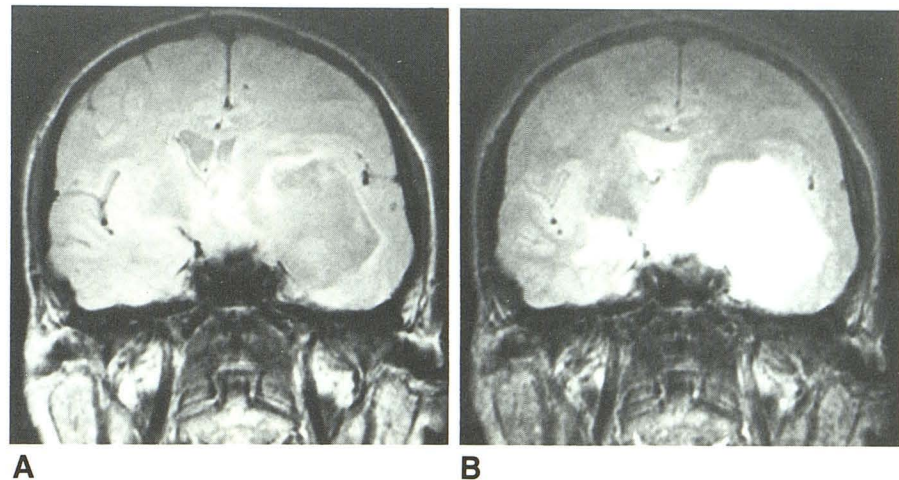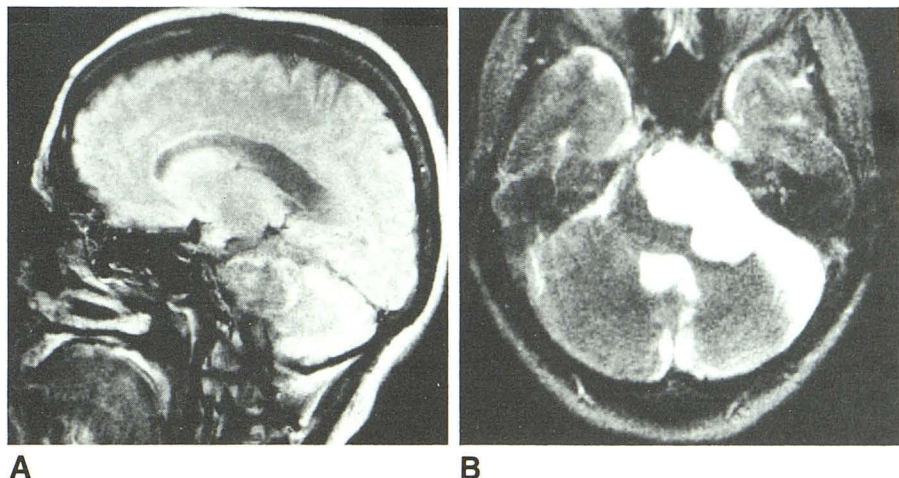

A

B

Fig. 3.—Case 8: this study was done on a 0.5-T unit.
A, In this intermediate-echo image, the lesion presents an inhomogeneous signal surrounded by a rim of hyperintense signal caused by CSF, which surrounds tumor.
B, In this second-echo image, lesion becomes completely hyperintense.

A

B

the subarachnoid space available before causing a mass effect. Moreover, their relation to the normal brain, the skull base, and the blood vessels could be evaluated. The coronal and sagittal views obtained with MR displayed the tumor in all their extension. The mass effect and the relation between the cysts and the deep cerebral structures could be better assessed because of the accurate anatomic detail obtained by MR in comparison with CT.

An evaluation of the circle of Willis and of the main arterial trunks at the skull base was possible with MR. The epider-

A   B

C   D
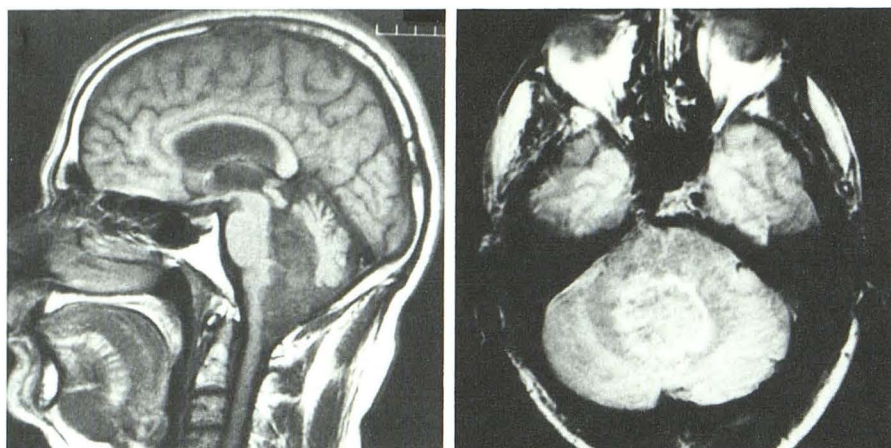
Fig. 4.—Case 7: epidermoid cyst located in fourth ventricle with a low extension through vallecular in cisterna magna.

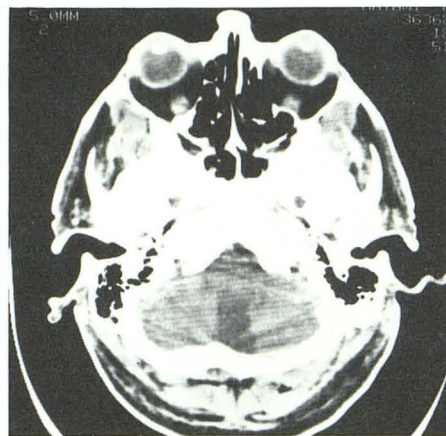*A,* T1-weighted MR image (550/30) shows lesion as hypointense.

B, In this intermediate-echo image, the lesion presents an inhomogeneous echo and is surrounded by a rim of high-intensity signal caused by encased CSF.

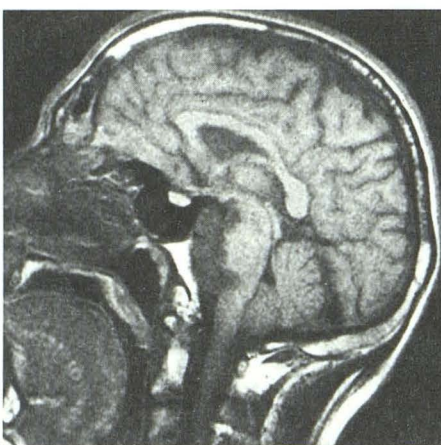*C,* In this second-echo image, the lesion becomes completely hyperintense.

D, CT scan does not reveal clearly the lower extension of tumor at level of vallecula.
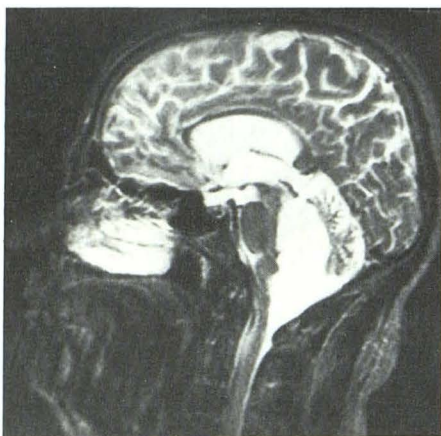
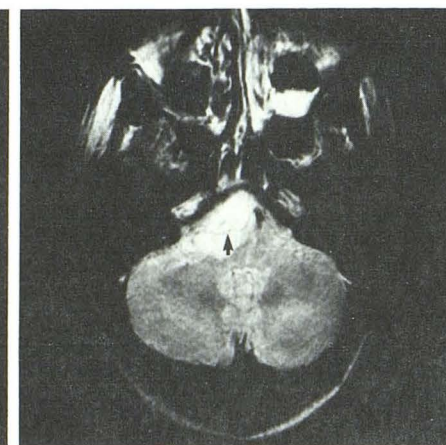

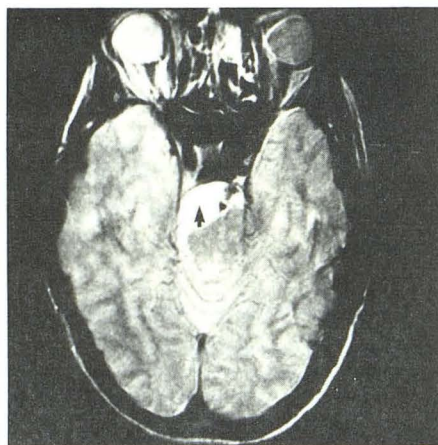

A   B   C

Fig. 5.—Case 5: lesion located at level of prepontine cistern and extending toward right cerebellopontine angle cistern.

A, In this T1-weighted MR image (550/30), lesion presents a low-intensity signal that increases in the T2-weighted images (*B* and *C*).

B and *C,* On these T2-weighted MR images (2100/60), the void signal, caused by anteroinferior cerebellar artery (*arrow* in *B*) and posterior superior cerebellar artery (*arrow* in *C*), is seen going through the tumor.

moid cysts tend to surround the arteries without obstructing them (Figs. 1 and 5). The vertebral angiogram obtained in case 3 showed only the indirect signs of a space-occupying lesion located in the fourth ventricle.

Discussion

Epidermoid cysts are slow-growing, benign tumors and, although they can reach a great size, they are usually very

well circumscribed. They occur more frequently in men than in women, between the ages of 40 and 60, and have a peak incidence in the fifth decade [7]. They can occur in either an extradural (20% of cases) or subdural (80% of cases) location [8]. Intracranially, they are usually situated in the cerebellopontine angle cisterns and in the middle cranial fossa. In 15% of cases they can be intraventricular, either in the atrium of the lateral ventricle or in the fourth ventricle [8].

Macroscopically, they are formed by an internal stratified squamous epithelium, which is covered by an external capsule. The cyst is filled by cholesterol crystals and other debris originating from the progressive desquamation of the epithelium. In particular, the cholesterol crystals are the result of the breakdown of the keratin [7–9]. In the literature, epidermoid cysts are reported to be characterized by long T1 and T2 relaxation times [10–18]. Our cases presented a similar character: they demonstrated a low-intensity signal on the T1 weighted images, an inhomogeneously iso- to hypointense signal on the intermediate echo, and a high-intensity signal on the second echo. Because epidermoid cysts are rich in cholesterol, one would expect them to have a high-intensity signal on the T1-weighted images; however, it is either the heterogeneity of their content [10] or the chemical state of the cholesterol itself that explains their relatively low signal on T1-weighted images. Specifically, the cholesterol in epidermoid cysts is in a solid state and therefore will differ in signal intensity from the cholesterol found in a liquid state, as in craniopharyngiomas.

Another hypothesis that could explain their long T1 and T2 relaxation time is their content of CSF, as was reported in a case of an epidermoid cyst filled with air during pneumoencephalography [19]. A mixture of cholesterol crystals, cell debris, and CSF could be responsible for the inhomogeneous signal on the proton-density images we observed in five cases. In the intermediate-echo images, five cases showed a thin, smooth rim of high-intensity signal that surrounded the tumor. In our opinion, this rim is consistent with CSF encased between tumor and parenchyma. This CSF presents high-intensity signal because of its slow motion compared with the CSF within the ventricles. The possibility that this signal represents edema seems unlikely, because the rim is too thin, smooth, and well-defined; and in all cases with a rim, CT showed no evidence of edema. In addition, epidermoid cysts do not usually cause edema [10].

MR was superior to CT for assessing the full extent of the lesions. The possibility of obtaining images free from bone artifact in all the anatomic planes is one of the major advantages of MR [12, 20]. In particular, the sagittal and coronal views allow assessment of the relationship and, eventually, of the mass effect of the tumor on the deep cerebral structures without the interfering density of the skull base. We also found that the epidermoid cysts adapt themselves to the surrounding subarachnoid spaces, and early in their course cause no mass effect on adjacent cerebral tissue.

MR allows the visualization of the main arterial trunks at the skull base and of the circle of Willis. The arterial vessels appear with a lack of signal, owing to the rapid blood flow [20]. The epidermoid cyst seems to surround the arteries without obstructing them. Finally, small vessels, such as the anteroinferior cerebellar artery, seem to run across the lesion. In two cases in our series the tumors presented a dumbell configuration, extending from the middle to the posterior cranial fossa. MR is the examination of choice in these cases because it allows the complete assessment of the lesions, and, thus, assists in planning the surgical approach. Finally, in the two cases in which the cysts were situated in the fourth ventricle, MR allowed the visualization of the full extent of the tumor. In particular, the lower part of the lesions, located in the vallecula, could be seen on MR, while CT at this level can be equivocal, owing to the presence of bone artifacts [20–22].

MR permits a better assessment of these lesions because it displays their relation to the brain and blood vessels (especially the arteries at the base of the skull). Although MR does not provide a specific image of epidermoid cysts, it is an invaluable tool for the evaluation of the full extent of the tumor and for presurgical planning.

REFERENCES

1. Picard L, Bernond C, Almeras M, Bracard S, Roland J. Aspects tomodensitométriques des kystes épidermoïdes intracraniens. *J Radiol* **1983**;84:529–535
2. Davis KR, Robertson GM, Taveras JM, New PFJ, Trevor R. Diagnosis of epidermoid tumor by computed tomography. *Radiology* **1976**;119: 347–353
3. Chambers AA, Lukin RR, Tomsick TA. Cranial epidermoid tumor by computed tomography. *Neurosurgery* **1977**;1:276–280
4. Dee RM, Kishore PRS, Young HI. Radiological evaluation of cerebellopontine angle epidermoid tumor. *Surg Neurol* **1980**;13:293–296
5. Fawcitt RA, Isherwood I. Radiodiagnostic of intracranial pearly tumors with particular reference to the value of computed tomography. *Neuroradiology* **1976**;11:235–242
6. Braun IF, Naidich TP, Leedo NE, Koslow M, Zimmermann MM, Chase NE. Dense intracranial epidermoid tumors. *Radiology* **1977**;122:714
7. Russell D, Rubinstein LJ. Congenital tumours of maldevelopmental origin. In: *Pathology of the nervous system*. Baltimore: Williams & Wilkins, **1977**:24–64
8. Lepoire J, Pertuiset J, eds. *Les kystes épidermoides cranioencéphaliques*. Paris: Masson et C., **1957**
9. Okezeki M, ed. *Fundamentals of neuropathology*. New York: Igaku-Shoin, **1983**
10. Vion-Dury J, Vincentelli F, Jiddane M, et al. MR imaging of epidermoid cysts. *Neuroradiology* **1987**;29:333–338
11. Davidson HD, Ouchi T, Steiner RE. NMR imaging of congenital intracranial germinal layer neoplasms. *Neuroradiology* **1985**;27:301–303
12. Gentry LR, Jacoby CG, Turski PA, Houston LW, Strother CM, Sackett JF. Cerebellopontine angle–petromastoid mass lesions: comparative study of diagnosis with MR imaging and CT. *Radiology* **1987**;162:513–520
13. Mawhinney RR, Buckley JH, Worthington BS. Magnetic resonance imaging of the cerebello-pontine angle. *Br J Radiol* **1986**;59:961–969
14. Rinck PA, Meindl S. Higer HP, Bieler EU, Pfannenstiel P. Brain tumors: detection and typing by use of CPMG sequences and in vivo T2 measurements. *Radiology* **1985**;157:103–106
15. MacKay IM, Bydder GM, Young IR. MR imaging of central nervous system tumors that do not display increase in T1 or T2. *J Comput Assist Tomogr* **1985**;9:1055–1061
16. Lee BCP, Kneeland JB, Deck MDF, Cahill PT. Posterior fossa lesions: magnetic resonance imaging. *Radiology* **1984**;153:137–143
17. Brant-Zawadzki M, Badami C, Mills CM, Norman PA, Newton M. Primary intracranial tumor imaging: a comparison of magnetic resonance and CT. *Radiology* **1984**;150:435–440
18. Latack JT, Kartush JM, Kemink JL, Graham MD, Knake JE. Epidermo-

idoma of the cerebello-pontine angle and temporal bone: CT and MR aspects. *Radiology* **1985**;157:361–366

19. Patriquin M, Melanson D, Bertrand G, Ethier R. Epidermoid tumours of the IV ventricle. *J Can Assoc Radiol* **1969**;20:35

20. Brant-Zawadzki M, Norman D. *Magnetic resonance imaging of the central nervous system.* New York: Raven, **1987**

21. Modic MT, Weinstein MA, Pavlicek W, Boumphrey F, Starnes D, Duchesneau PM. Magnetic resonance imaging of the cervical spine: technical and clinical observations. *AJNR* **1984**;5:15–22, *AJR* **1983**;141:1129–1136

22. Scotti G, Scialfa G, Tampieri D, Landoni L. Magnetic resonance imaging of the posterior fossa. In: Valk J, ed. *Neuroradiology.* Amsterdam: Elsevier, **1986**:43–54